Electron Beam Mediated Crosslinking of Blown Film Extruded Biodegradable PGA/PBAT Blends towards High Toughness and Low Oxygen Permeation

Paresh Kumar Samantaray [$a#], Christopher Ellingford [a#], Stefano Farris [b], Donal O'Sullivan [c], Bowen Tan [d], Zhaoyang Sun [d], Tony McNally*[a], Chaoying Wan*[a]

[a] International Institute for Nanocomposites Manufacturing (IINM), WMG, University of Warwick, CV4 7AL, U.K.

[$] Present address: Division of Chemistry and Chemical Engineering, California Institute of Technology, 1200 E. California Blvd., Pasadena, California, 91125, USA

[b] Department of Food, Environmental and Nutritional Sciences, University of Milan, 20133, Milano, Italy

[c] Sherkin Technologies UK Ltd., Daresbury Innovation Centre, WA4 4FS, UK.

[d] PJIM Polymer Scientific Co., Ltd., Shanghai, 201102, China

*Corresponding authors: t.mcnally@warwick.ac.uk; chaoying.wan@warwick.ac.uk

[#] Equal contribution

Abstract

Due to its high crystallinity, tailored compostability, and superior barrier performance, poly(glycolic acid)(PGA) has great potential as a substitute for current single-use plastics used in food packaging applications and with a lower carbon footprint. However, its susceptibility to hydrolysis and mechanical brittleness hinders its direct suitability in packaging. In this work, we circumvent this limitation by first blending PGA with a thermoplastic polyester, poly (butylene adipate-co-terephthalate) (PBAT), and a glycidyl crosslinker via industrial-scale twin-screw extrusion and then converting to film by blown film extrusion. The surface of the films was then chemically crosslinked using electron-beam treatment (EBT) to impart excellent barrier properties. Here, the electron beam plays a dual role. Firstly, it crosslinks the surface of the films and improves the oxygen and moisture barrier performance, both improved due to blending with PBAT. Secondly, it doesn't compromise the toughness or extension at the break, both desirable for flexible packaging applications. A dosage of 250 kGy EBT resulted in the film having an oxygen barrier permeation of 57.0-59.8 cm^3 mm m^{-2} 24 h^{-1} atm^{-1} and a water vapor permeation of 26.8 g m^{-2} 24 h^{-1} while maintaining a high toughness of 75 MPa. At dosages higher than 300 kGy, inhomogeneities formed on the surface of the films, and some degradation in the mechanical properties of the films is observed. This work highlights the possibility of deriving superior biopolymer barrier performance while retaining the mechanical properties required for food packaging using a combination of blending and electron beam treatment, both scalable processes.

Keywords: electron beam treatment; blown film extrusion; barrier films; Polyglycolic acid blend; compostable food packaging;

Introduction

Petrochemical-derived plastics such as poly(ethylene) (PE), poly(propylene) (PP), and poly(ethylene terephthalate) (PET) have been extensively used in packaging applications due to their intrinsic superior mechanical strength and highly selective gas barrier properties for oxygen and water vapor. This is important for protecting the packaging contents, preventing spoilage, increasing shelf-life, and for protection whilst transporting from growers to consumers.[1] With the global production of plastics at approximately 400 million metric tonnes per annum, and predictions for this to double by around 2040, if our relationship with plastics is maintained,[2] the issues relating to waste and reliance on crude oil sources will become even more critical to resolve. Furthermore, due to poor segregation and recycling options, a large proportion of these plastics end up in landfills,[3] which hinders closing the plastic recycling loop. Single-use plastics are currently the key drivers to this current problem because of their short-intended usage cycle. Hence, polymer materials that incorporate elements of increased sustainability or biodegradability and investigations into zero waste through a circular economy have become the focal point of intensive research due to increasing government regulations and increased societal demand for a change to the status quo.[3]

In this regard, biodegradable polymers such as poly (lactic acid) (PLA) and poly (butylene adipate-co-terephthalate) (PBAT) have been investigated intensively,[4-9] with the former for its high mechanical strength for rigid packaging applications and the latter for its flexibility. However, a common issue limiting these biodegradable polymers is their high susceptibility for oxygen and water vapor permeation, critical for specific packaging applications, e.g., for coffee, dairy powder, meat, and perishable produce where spoilage collates directly with barrier requirements.[1, 10] High water permeation introduces additional problems as it can accelerate hydrolytic degradation of the polymers,[11] decreasing the barrier properties further and compromising the usable shelf-life of the material. Materials like PBAT are also environmentally friendly with no demonstrated ecotoxic or phototoxic effects on plants like radish, monocotyledonous oat, cress, lettuce, and onion, to name a few, and have also had no in-vitro cytotoxicity to mammalian cell lines as well.[12-13]

To improve gas barrier properties, blending of polymers, where one possesses high mechanical performance, and the other possesses high barrier performance, such as blending of PLA/ poly(butylene succinate (PBS)[14], PLA/poly(3-hydroxybutyrate-co-3-hydroxyvalerate) (PHBV), and PBAT/ poly(propylene carbonate) (PPC), is one such approach. However, typically such polymer systems are immiscible and require the addition of a compatibilizer (e.g., small compounds, nanoparticles, or a compatibilizing third polymer, including copolymers of the polymer blend components). For example, 3 phr an epoxy-terminated branched polymer was utilized to generate *in-situ* PLA, and PBAT branched

copolymers for compatibilization of 70/30 PLA/PBAT, which resulted in an increase in the strain at break from 45.8 % to 272 % and improving the impact strength from 26.2 kJ m^{-2} to 45.3 kJ m^{-2} [15], relative to the uncompatabilized blend. Alternatively, PLA and PBAT polymer chain end groups can also be reacted with linear chain extenders to form *in-situ* copolymers. Phthalic acid and 2,2'-(1,3-phenylene) bis(2-oxazoline) were able to compatibilize a PLA/PBAT 80/20 blend through increased interfacial adhesion between blend components. This resulted in blends with high strength (45.3 MPa) and high strain at break (516%).[16] Finally, ethylene methyl acrylate – glycidyl methacrylate copolymer (EMA-GMA) has been used to form super-tough PLA/PBAT blends when 15 wt.% is added, leading to a strain at break of 278% and impact strength of 61.9 kJ m^{-2}, due to a core-shell PBAT structure and a co-continuous PLA/EMA-GMA phase morphology.[17]

Polyglycolic acid (PGA) is structurally analogous to PLA, with the exception of a branched methyl group adjacent to the in-chain ester group.[18] However, it exhibits significantly greater oxygen and water vapor barrier properties in comparison,[1] in part due to its high crystallinity and linearity.[19-20] PGA breaks down into its monomeric units (glycolic acid) which is a natural metabolite which is directly taken up by mammalian cells making it a green and eco-friendly material. [19] Its brittleness and narrow processing window make it suitable for rigid packaging applications when unmodified. However, owing to the chemical similarities between PGA and PLA, chemical routes by which the extension at break is tailored in PLA can be possibly attempted for PGA, effectively to yield flexible polymer blends. Wang *et al.* blended different ratios of PGA and PBAT together and compatibilized *in-situ* through 4,4'methylenebis (phenyl isocyanate)(MDI) acting as a chain extender compound for both PGA and PBAT. The enhanced impact strength of the blend was greatest for 70/30 PBAT/PGA with 0.5% MDI at 56.6 kJ m^{-2}.[21] In a different study, Shen *et al.* used a chain extender ADR 4370s to compatibilize different ratios of PGA and PBAT. For 65/35/0.9 PBAT/PGA/ADR 4370s, the extension at break was 498.1 ± 22.9 % while, the oxygen permeability was 3.28 x 10^{-14} (cm^3. cm) /cm^2 .Pa.s).[22] Very recently, Ellingford and Samantaray *et al.* used a terpolymer of ethylene, methyl acrylate, and glycidyl methacrylate (EMA-GMA) (commercially Lotader AX8900) to compatibilize 50/50 PGA/PBAT blends for packaging applications. A loading of 20 wt.% EMA-GMA improved the extensibility of 50/50 PGA/PBAT blends from 10.7 % to 145 % while reducing the oxygen permeability from 125 to 103 (cm^3. mm)/ (m^2 24 h. atm) with a ~47 % improvement in water vapor barrier properties.[18] When Niu *et al.* blended 1 wt. % EMA-GMA modified PBAT with PGA in 30/70 ratio (with PGA being the major component), elongation at break of 45 ± 4 % and notched impact strength of 14.4 ± 1.6 kJ/m^2. Pristine PGA demonstrated 4.8 % elongation at break and a notched impact strength of 3.5 kJ/m^2. [23]

Surface modification strategies like electron beam treatment (EBT) have immense potential to improve gas barrier performance further. In EBT, highly energetic electrons are emitted via a vacuum tube under a strong electric field. The treatment is versatile, scalable, and can be controlled by three

parameters: the depth of electron penetration in the substrate (keV), the throughput of the electron beam (kW), and the dosage of electrons (kGy) on the substrate. In the EBT treatment process, during the irradiation of polymer films, reactive species such as ions and oxygen radicals are generated, which are sufficiently energetic to cause reactive grafting and/or create crosslinks between functional moieties present on the polymer chains of irradiated surfaces.[24] By varying the dosage of the electrons, the extent of this reaction can be controlled. At lower dosages, the e-beam is capable of dislodging atoms from the polymeric chains as well as crosslink available oxygen functionalities due to the reaction of oxygen radicals with the moieties. At higher dosages, the beam is sufficiently energetic to cause chain scission and degradation of polymer surface under irradiation. Scheme 1 provides a schematic overview of the overall EBT process. The crosslinking formed from this process reduces the polymer matrix free volume,[25] enhancing the gas barrier properties. Further, the wettability of the surface is also enhanced by this treatment.[24] However, the dosage of electrons must be carefully controlled to ensure that degradation does not occur. Kita *et al.* investigated the effect of EBT on polypropylene (PP), polybutadiene (PB), and polyethylene terephthalate (PET) with respect to various gases. Whilst polymers such as PET were insensitive to the treatment, the gas barrier properties of PP and PB were enhanced.[25]

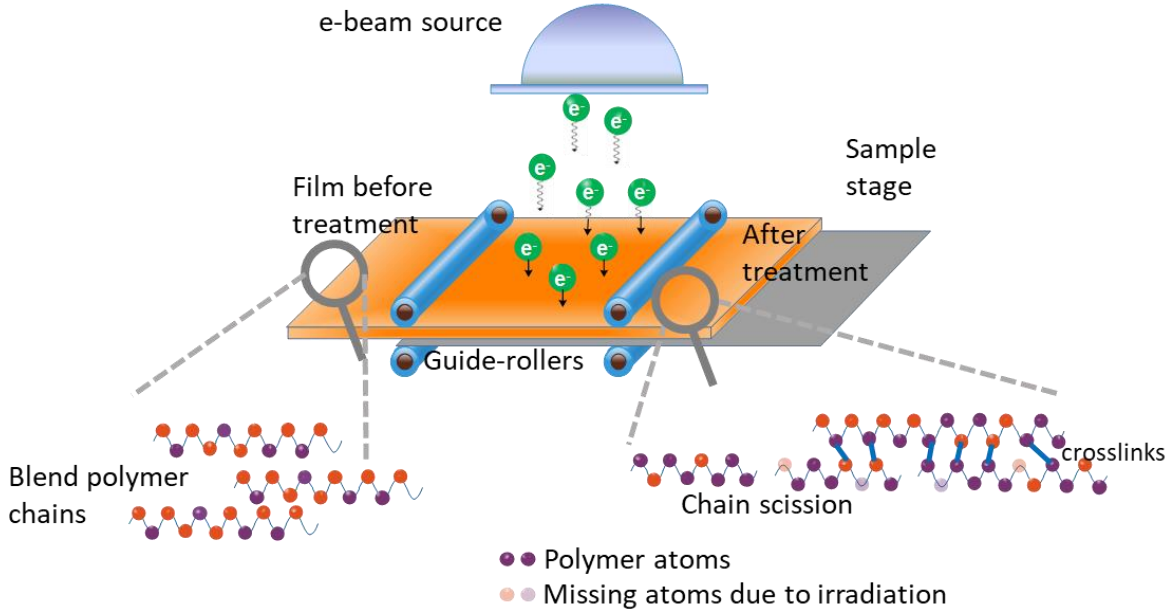

Scheme 1. Schematic representation of EBT for crosslinking of polymers. It should be noted that chain scission and degradation only occur at higher e-beam dosages while crosslinking is observed for lower dosages during EBT.

This work uses a synergistic combination of reactive compatibilization of PGA/PBAT blends with glycidyl methacrylate (GMA) as a compatibilizer followed by post-processing blown films then using EBT treatment to yield a biodegradable blend in film form with excellent gas barrier properties and relatively unperturbed elongation at break for packaging applications. We investigate blends of

PGA and PBAT in a 20/80 (w/w) ratio, reactively compatibilized through the addition of 2 wt. % GMA and convert into films. The films were surface treated with EBT at a constant voltage (150 kV) and variable dosages up to 450 kGy and their effect on the mechanical and physical properties investigated, and the gas barrier properties to oxygen and water vapor permeation were evaluated. Our work aims to advance low permeation biodegradable polymers for film packaging applications as alternatives for commonly single-use non-degradable polymers.

Experimental

Materials

Poly (glycolic acid)(PGA) was supplied by PJIM Polymer Scientific Co. Ltd with a number average molecular weight of 10^5 g mol^{-1}. PBAT (Ecoflex Blend F C1200) was obtained from BASF with a number average molecular weight of 1.42×10^5 g mol^{-1}. Glycidyl methacrylate (GMA, 97 %) was procured from Sigma Aldrich.

Blend and blown film preparation

PGA and PBAT were dried overnight at 65 °C in a desiccant dryer before use. PGA/PBAT (20/80) blends were melt mixed with 2 wt. % GMA using a TSE 24mm twin-screw extruder with an L/D ratio of 40:1. The temperature of the different portions of the extruder was set chronologically with feed zones as 150, 160, and 180 °C, the compression zones with 190, 210, and 220 °C, and the metering zone as 230 °C. The die output was set at 190 °C. The screw speed and feed rate were set to 110 rpm and 22 %, respectively. The strands were chopped and dried in a desiccant dryer overnight at 80 °C to remove moisture, which can hinder film blowing. Films of nearly ~100 µm thickness were obtained by blown film extrusion using a Killion (Davis Standard) line at 190 °C and a 2.5 m/min take-up speed.

Electron Beam Treatment

Electron Beam Treatment (EBT) was performed using an EBLab200 system from ebeam Technologies, Switzerland, conducted at Sherkin Technologies UK Ltd, UK. 15 cm x 15 cm pieces of the polymer blend films were cut and preheated to 60 °C before treatment in air at 9 m s^{-1}. The beam energy used for the treatment was maintained at 150 keV, with the electron beam dosage varied from 90 kGy up to 450 kGy. The samples were then stored under a vacuum to prevent hydrolytic degradation.

Characterization

Attenuated total reflection-Fourier Transform Infrared Spectra (ATR-FTIR) were recorded using a Bruker Tensor 27 instrument in the wavenumber range between 650 cm^{-1} and 4000 cm^{-1}, at a resolution

of 2 cm^{-1} with a background of 32 scans and a sample scan of 64 scans. FTIR spectra referred throughout the text means ATR-FTIR. Differential Scanning Calorimetry (DSC) was performed using a Mettler Toledo DSC STAR1, with 5 – 8 mg of sample in a 40 µl aluminum DSC pan under a constant N_2 flow of 50 mL min^{-1}. A heating and cooling rate of 10 K min^{-1} between -60 °C to 245 °C was used for two heating and two cooling cycles. Tensile testing was performed using a 250 kN static Instron tensile tester with a 1 kN load cell and grips, and samples conforming to ASTM D638 were tested at a rate of 10 mm min^{-1} until 110 % strain and, then at 25 mm min^{-1} until sample failure. Contact Angle measurements were recorded using an Attension Theta Lite system with 2.5 µL droplets of deionized water as the wetting solvent. The contact angle measurements were recorded for 10 seconds at a frame rate of 51 FPS and repeated five times for each sample before calculating the average contact angle from each run. The oxygen transmission rate (OTR) and water vapour transmission rate (WVTR) were measured using a Permtech Totalperm Permeabilimeter following ASTM 3985 (OTR @ 23 °C/0% RH), ASTM F1927 (OTR @ 23 °C/50 % RH) and ASTM F1249 (WVTR @ 23 °C/65% RH). The variability in film thickness was negated by converting the OTR and WVTR to permeability coefficients $P'O_2$ (cm^3 mm m^{-2} $24h^{-1}$ atm^{-1}) and P'WV (g mm m^{-2} $24h^{-1}$ atm^{-1}).

Results and Discussion

PGA/PBAT extruded blown films were compatibilized by adding GMA, where the epoxy groups react with both the hydroxyl and carboxyl chain end groups of PGA and PBAT.[18, 26] The reaction of GMA to a macromolecular can progress via transesterification and epoxide ring opening mechanism.[27] This is confirmed from FTIR, see Figure 1, by the disappearance of the carbonyl stretch of GMA at 1638 cm^{-1} and the disappearance of the asymmetric and symmetric C-O-C stretches at 907 cm^{-1} and 843 cm^{-1}, respectively, indicating that PGA/PBAT copolymers had been formed *in-situ* and functioning as a compatibilizer. Similar reaction of the glycidyl moieties have also been observed by Coiai *et al*.[28] and Kumar *et al.* [26] 2 wt% GMA was selected as the optimal quantity of compatibilizer based on optimization not shown here.

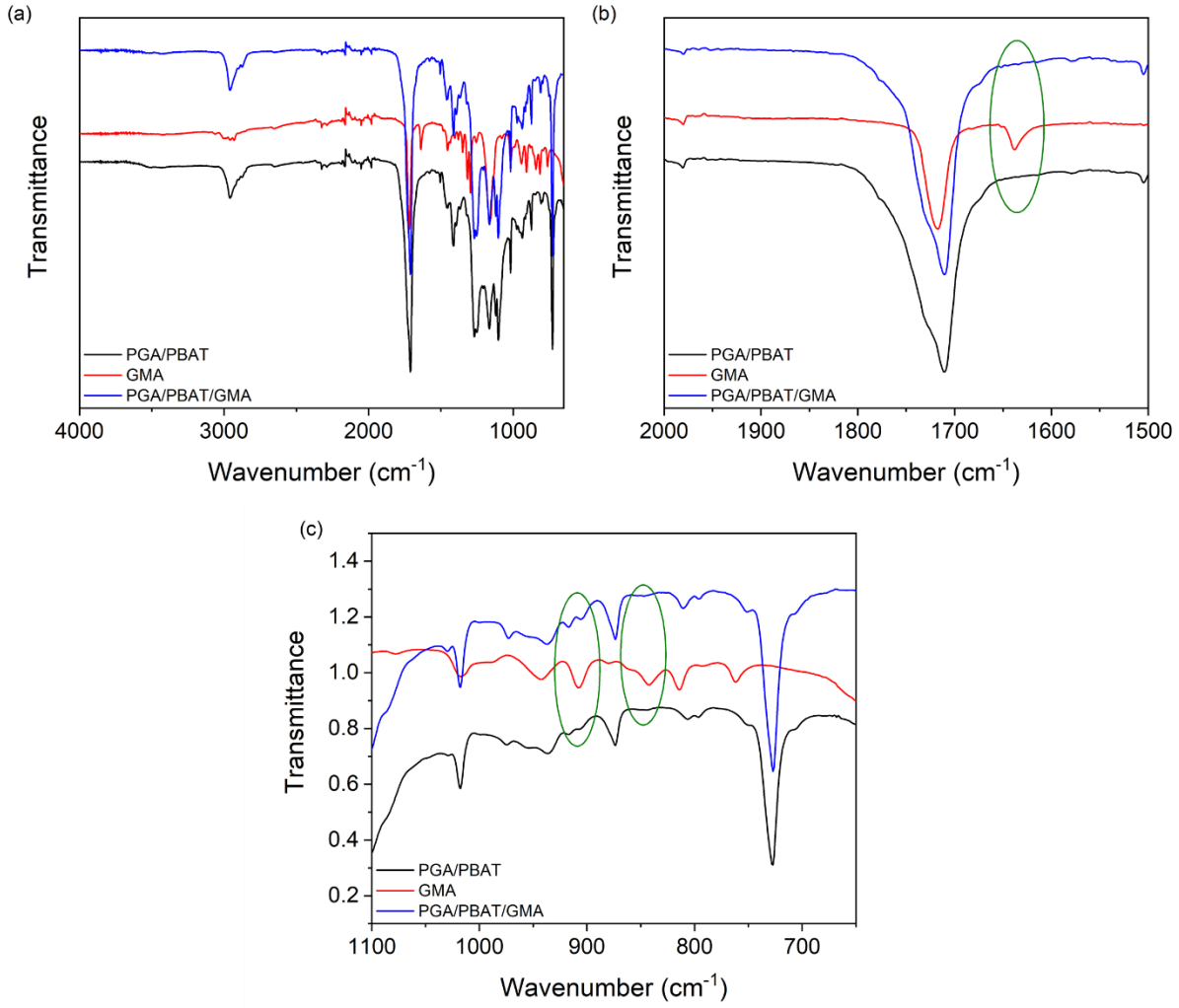

Figure 1. FTIR spectra for PGA/PBAT, GMA, and PGA/PBAT/GMA. (a) the full FTIR spectrum in the range 4000 – 650 cm^{-1}, (b) the spectrum highlighting the disappearance of the carbonyl peak, and (c) the disappearance of the epoxide asymmetric and symmetric C-O-C stretch.

Following this, the application of EBT on the PGA/PBAT/GMA blown films with dosages up to 450 kGy was applied to the film surface to induce crosslinking of the polymer chains with a view to enhancing gas barrier properties. Visible differences in the polymer films were observed with treatment beyond 300 kGy, culminating in large solid white regions randomly distributed across the film surface. This was most striking for the films treated at 350 kGy, with further increases in dosage increasing the regularity of the film inhomogeneity (*i.e.*, smaller yet, more uniform white regions). SEM imaging shows the increase in degradation on the polymer film surface because of increased dosage during EBT (see Figure S2) the blend phase morphology of PGA/PBAT and PGA/PBAT/GMA films are shown in Figure S3.

To investigate the inhomogeneity of the polymer films treated above 300 kGy, FTIR analysis of the EBT films is shown in Figure 2 and Figure S1. Overall, all the spectra show identical key features, i.e., the ester C=O stretch at 1710 cm^{-1} from PGA and PBAT; C-H bending at 1460 – 1300 cm^{-1}, asymmetric

C-O-C stretch at 1260 cm^{-1} for PBAT, symmetric C-O-C stretch for PBAT, and asymmetric C-O-C stretch for PGA at 1100 cm^{-1} and a symmetric C-O-C stretch for PGA as a shoulder peak at 1070 cm^{-1}. The uniformity of the spectra across the sample range indicates that critically complete degradation of the film surface did not occur. However, the C=O stretch for films treated with 300, 350, and 400 kGy indicated some degradation and chain scission had occurred as the formation of anhydride shoulder peaks at 1750 – 1780 cm^{-1} was evident. (Encircled regions in figure 2.) These are attributed to the degradation of the esters along the polymer chain backbone and indicate the formation of oxidatively degraded chain scission with terminal carboxylic acids and anhydrides. (See Scheme 1) This follows previously observed degradation above 250 kGy EBT of other polymers.[29-31] The FTIR spectra of the white regions of the films treated at 450 kGy or the other areas of the films treated with 400 and 450 kGy do not show any degradation. This is presumably because after significant irradiation of the film at higher dosages, sufficient scission, crosslinking, and degradation occurs on the polymer surface. The electron beam and the oxygen radicals generated would have either scavenged and/or crosslinked the available functional moieties present on the surface. Hence, no further perturbations are observed.

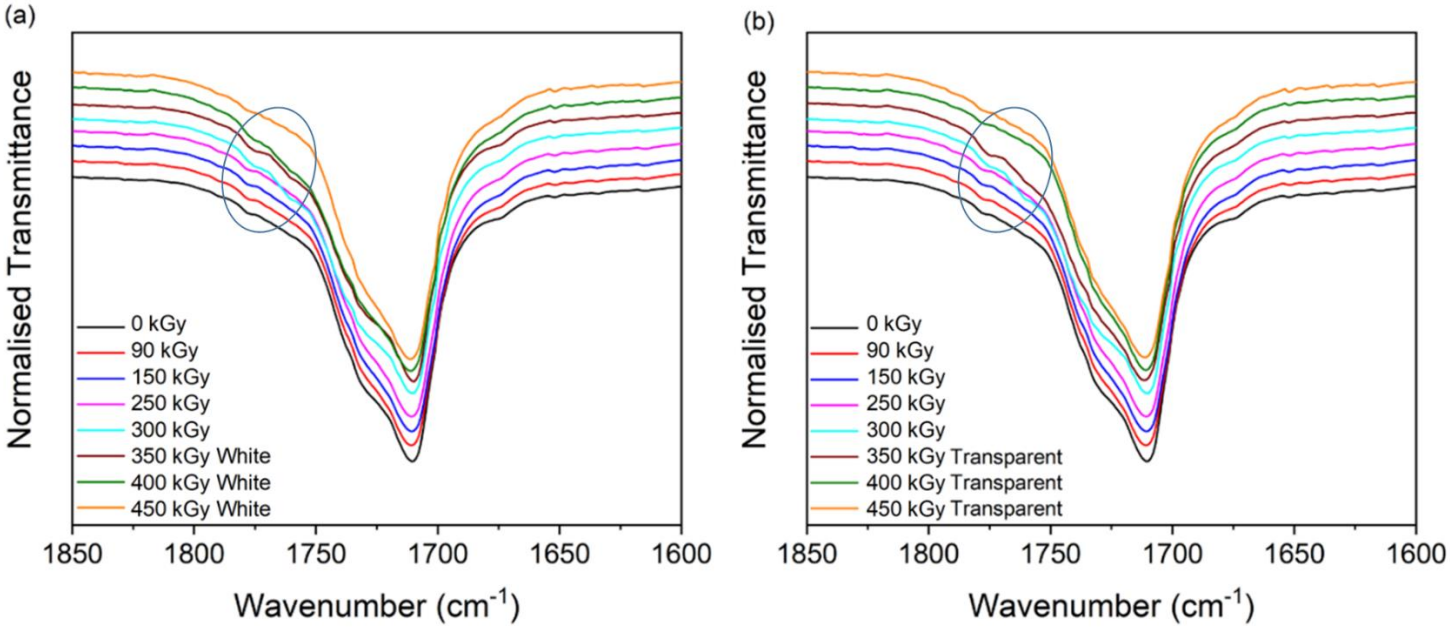

Figure 2. FTIR of C=O ester peak for electron beam treated PGA/PBAT/GMA films for (a) white regions of inhomogeneity and (b) transparent regions of inhomogeneity between 0 – 450 kGy dosages

The effect of EBT on the crystallinity of the polymer films was investigated using differential scanning calorimetry (DSC), and the relevant thermal parameters were determined (Figure S4) and are listed in Table 1. These parameters were determined from the first heating and cooling cycles, with the equivalent listed for the second heating cycle in Table S1. Whilst the first heating cycle also includes the thermal history of the polymer blend, PGA did not show a crystallization peak, and from the second heating cycle, the PGA was only 1 ~ 2 % crystalline due to the slow formation of PGA crystallite

structures. As the electron beam dosage increases from 90 kGy to 300 kGy, a decrease in the $\%X_c$ for PBAT is primarily observed, indicating that irradiation caused possible crosslinking that restricts PBAT chains from crystallizing. Once the white discontinuities form, a distinct difference in the $\%X_c$ of PBAT is observed. Typically, the white regions now have a PBAT $\%X_c$ of 21, whereas for the non-white regions, $\%X_c$ = 13 ~ 15. Furthermore, a lower melting temperature (T_m) is observed in the more crystalline white regions of PBAT. This variation in X_c on the surface of the films was not observed in the DSC curves for the first cooling or second heating cycles, nor were differences in the glass transition temperature (T_g) and crystallization temperature (T_c) of the polymer blends. Comparatively, EBT had a minimal effect on the $\%X_c$ and T_m of PGA regardless of the dosage applied. This indicates that crosslinking and subsequent degradation from electron beam treatment were primarily located in the PBAT phase of the polymer blend.

Table 1. Thermal parameters, including the glass transition temperature (T_g), melting temperature (T_m), percentage crystallinity ($\%X_c$), and crystallization temperature (T_c) for PGA, PBAT, and EBT PGA/PBAT/GMA films, determined from DSC measurements.

Sample	First Heating Cycle						First Cooling Cycle			
	PGA			PBAT			PGA		PBAT	
	T_g (°C)	T_m (°C)	$\%X_c$	T_g (°C)	T_m (°C)	$\%X_c$	T_c (°C)	$\%X_c$	T_c (°C)	$\%X_c$
PGA	52.03	225.24	42.88	-	-	-	192.70	46.4	-	-
PBAT	-	-	-	-28.68	117.31	20.13	-	-	75.90	15.90
PGA/PBAT	40.92	207.96	31.60	-35.04	108.02	26.86	181.15	2.78	97.81	16.57
0 kGy	39.73	219.79	68.07	-29.89	124.80	13.33	-	-	72.83	18.63
90 kGy	40.24	216.69	39.41	-28.22	117.32	25.47	-	-	73.14	18.04
150 kGy	39.74	215.37	37.61	-29.88	115.34	23.07	-	-	73.96	23.04
250 kGy	39.38	212.80	37.85	-30.39	106.13	21.13	-	-	74.68	18.16
300 kGy	41.26	216.28	37.83	-27.70	111.22	12.23	-	-	67.28	24.54
350 kGy **White domain**	40.61	214.5	37.8	-28.36	106.91	21.62	-	-	67.59	24.39
350 kGy **Transparent domain**	44.77	214.98	35.67	-24.86	111.07	15.46	-	-	66.26	23.49

400 kGy **White domain**	40.45	214.18	34.93	-27.69	106.91	20.54	-	-	67.25	24.7
400 kGy **Transparent domain**	45.27	213.83	36.84	-26.20	115.74	13.54	-	-	65.93	23.77
450 kGy **White domain**	43.10	214.45	34.12	-26.87	107.71	21.60	-	-	66.28	24.21
450 kGy **Transparent domain**	44.42	214.12	36.41	-25.87	110.38	14.57	-	-	64.62	24.09

The effect of the crosslinking and degradation on the tensile mechanical properties of the polymer blends is shown in the representative stress-strain curves in Figure 3, with the average values for tensile strength (σ), Young's modulus (E), strain at break (ε_{max}) and tensile toughness listed in Table 2. Overall, it can be seen that the effect of crosslinking from EBT increases the tensile strength of the polymer blend with increasing EBT dosage up to 250 kGy, from 15.8 MPa to 18.1 MPa, while Young's modulus is unchanged. A small decrease in the strain at break is observed due to the increase in crosslinking, and as a result, the toughness of the polymer blend only increases marginally. However, for an EBT dosage of 300 kGy, a large decrease in mechanical performance is obtained, i.e., a decrease in the strain at break and tensile strength decreasing from 541 % to 406 % and from 18.1 MPa to 14.4 MPa, when the dosage was increased from 250 to 300 kGy. Consequently, this results in a large decrease in the toughness of the blend with increasing EBT dosage from 250 kGy to 300 kGy, from 75.3 MPa to 45.2 MPa, respectively. Furthermore, the effect of EBT induced degradation of the polymer film surface on E is clearly observed at 400 kGy and 450 kGy, where a reduction from 111.9 MPa to 93.2 MPa and then to 84.6 MPa was recorded.

Table 2. Tensile mechanical properties of PGA/PBAT/GMA blends as a function of different dosages applied during electron beam treatment.

Dosage (kGy)	**Young's Modulus, E (MPa)**	**Tensile Strength, σ (MPa)**	**Strain at break, ε_{max} (%)**	**Tensile Toughness (MPa)**
0	108.2 ± 54.1	15.8 ± 2.1	577.5 ± 91.9	74.4 ± 16.4
90	117.1 ± 13.2	17.5 ± 1.7	520.5 ± 79.4	71.4 ± 15.4
150	108.2 ± 6.9	17.2 ± 1.6	528.6 ± 74.7	71.3 ± 13.6
250	107.2 ± 13.9	18.1 ± 1.6	541.2 ± 52.4	75.3 ± 11.7
300	100.7 ± 9.4	14.4 ± 0.76	406.4 ± 44.8	45.2 ± 7.1

350	111.9 ± 18.4	14.3 ± 0.79	368.9 ± 55.8	37.9 ± 8.9
400	93.2 ± 9.5	15.0 ± 1.14	394.9 ± 49.6	40.9 ± 5.3
450	84.6 ± 21.0	13.7 ± 0.90	312.4 ± 40.0	29.6 ± 4.9

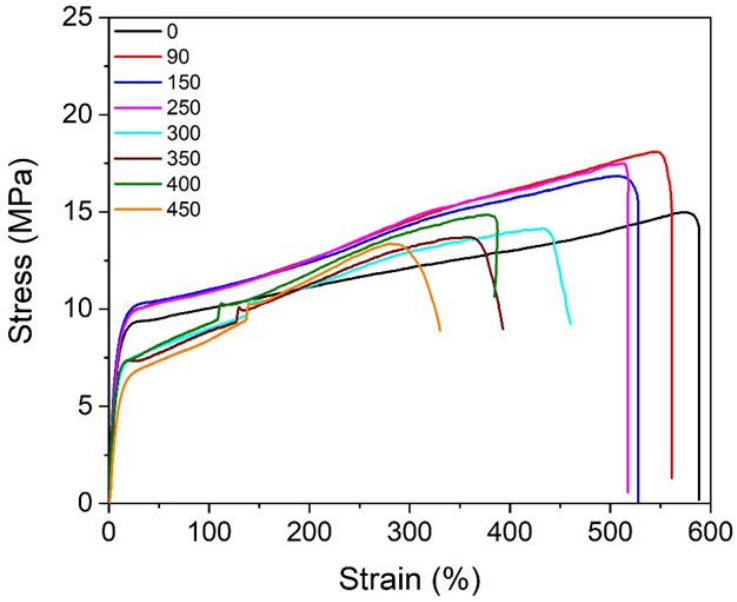

Figure 3. Representative stress-strain curves for PGA/PBAT/GMA films as a function of dosage applied during electron beam treatment. (Units for the legend are in kGy)

The contact angle of the films post EBT was determined to examine the effect of crosslinking, see Figure 4, on the surface wettability of the polymer blends. The application of EBT resulted in an increase in the hydrophilicity of the polymer blend films, observed from a decrease in the contact angle. Unmodified PGA/PBAT/GMA blends exhibited a contact angle of 75.7°, which decreased to 64.6° upon increasing the EBT dosage to 250 kGy. However, a dosage of 300 kGy resulted in an increase in surface hydrophobicity, observed from an increase in the contact angle to 74.6°. This pattern has been observed previously, including for PLA.[32-33] We hypothesize that the increase in hydrophobicity results from complete utilization of the functional moieties like anhydrides generated as seen in the FTIR spectra in Figure 2 that contribute to hydrophilicity and formation of non-functional alkyl derivatives, and surface rearrangement from increased crosslinking.

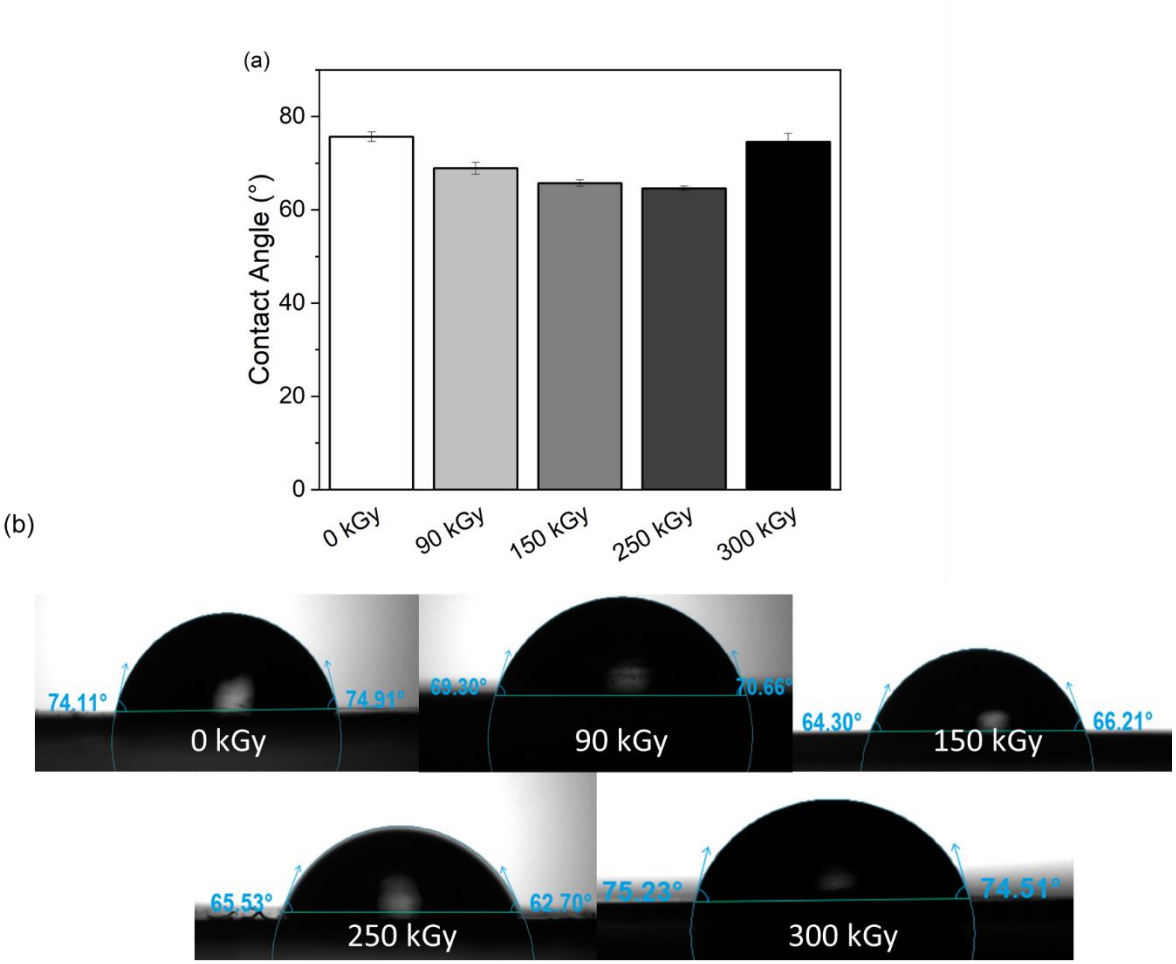

Figure 4. (a) Contact angle values and (b) images of the droplet from contact angle measurements of PGA/PBAT/GMA blends after EBT at dosages up to 300 kGy.

An investigation into the gas barrier properties of the EBT films was conducted by investigating their permeability to oxygen and water. In film packaging, maintaining an effective barrier to water and oxygen is important for preserving short shelf-life goods and preventing food spoilage and wastage. Table 3 lists commonly used flexible and rigid food packaging materials, with the results from this work included. Neat PGA is reported to have both low oxygen and water vapor permeability, whilst the PBAT used in this work had a high oxygen permeability but a low water vapor permeability. Prior to surface crosslinking, the PGA/PBAT/GMA film had an oxygen permeability (P'O_2) of 71.1 – 74.3 cm^3 mm m^{-2} 24 h^{-1} atm^{-1} and a water vapor permeability (P'WV) of 24.3 g mm m^{-2} 24 h^{-1}, highlighting excellent oxygen gas barrier properties, although greater permeability for water vapor. The application of EBT at 90 kGy resulted in a 12 % decrease in oxygen permeability, down to 62.8 – 65.7 cm^3 mm m^{-2} 24 h^{-1} atm^{-1}. The changes in crystallinity obtained rationalizes this behavior for the polymer films, where the $\%X_c$ for the PBAT region increased whilst the $\%X_c$ for the PGA region decreased, resulting in a net increase in polymer blend crystallinity. A small increase in the P'WV is potentially from after-treatment surface defects due to oxygen radical interactions generated during the EBT process, corresponding to

the defects observed from SEM imaging (Figure S2) and the increased hydrophilicity observed from contact angle measurements (Figure 4), and the published literature.[24] As electron beam dosage increased to 250 kGy, the oxygen permeability decreased to 57.0 – 59.8 cm^3 mm m^{-2} $24h^{-1}$ atm^{-1} despite a decrease in PBAT crystallinity, indicating the EBT induced surface crosslinking was responsible for the decrease in oxygen permeability. However, the application of 300 kGy during EBT did not further increase the gas barrier properties of the film. Instead, the $P'O_2$ increased to 69.5 – 73.2 cm^3 mm m^{-2} 24 h^{-1} atm^{-1}, linked to both the decrease in the $\%X_c$ of the PBAT regions and possibly surface rearrangement due to the formation of degradation products. Table S3 shows the gas barrier properties for the films treated with a dosage of 350 kGy and greater. As can be seen, no further improvements in $P'O_2$ were observed. Overall, this shows that both the oxygen and water vapor permeability were significantly enhanced, and the resulting polymer blends have a 'medium' barrier grade classification,[1] while retaining flexibility and stretchability. Figure 5 provides a comparison of the OTR and WVTR for different barrier films for food packaging with our results. It can be observed that our modified film is suitable for packaging bakery products as well as salads, fresh fruits, and vegetables. Figure 6 discusses the overall results obtained from the e-beam experiments. In brief, low dosages of 90-150 kGy generated oxygen radicals and knocked some atoms in the polymer chains to cause chemical crosslinking. This resulted in increased hydrophilicity while no differences in the films' mechanical or P'O2 or P'WP. At 250 kGy dosage, lowest hydrophobicity was observed and the mechanical properties were comparable to the unmodified films. Interestingly, this dosage was the sweet spot giving lowest OTR and WVTR. Increasing the dosage further caused surface degradation of films visibly and resulted the films to become hydrophobic compared to previous dosage films. Reduction in strain at break and tensile toughness possibly indicated that the chain scissions and polymer degradation was accelerated at 300 kGy or higher dosages. Increase in the OTR was also observed which is undesirable from packaging perspective.

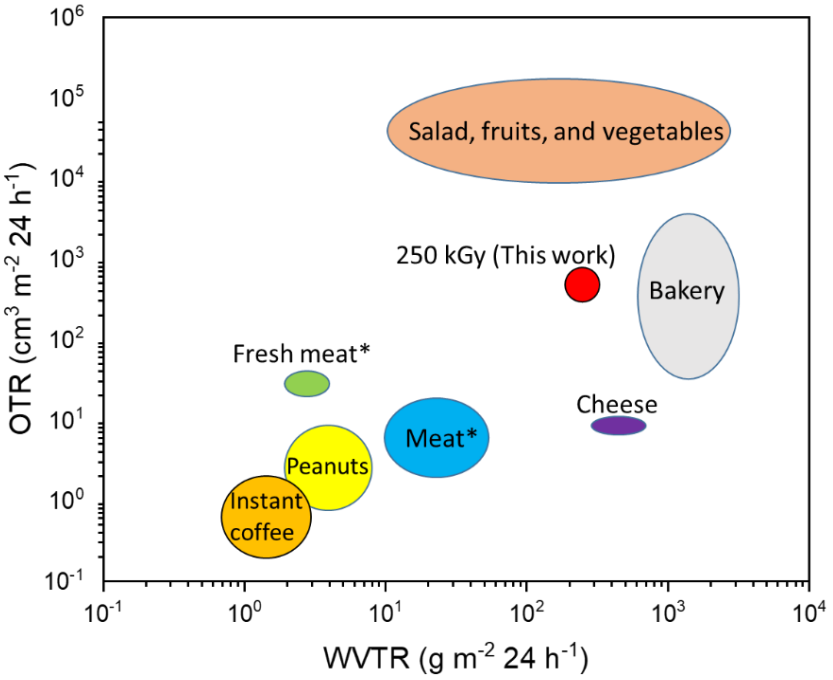

Figure 5: OTR and WVTR requirements of barrier films in selected food applications in comparison with the values measured for EBT films produced in this work. (* indicates modified atmosphere packaging.) Data extracted and re-plotted from reference[34]

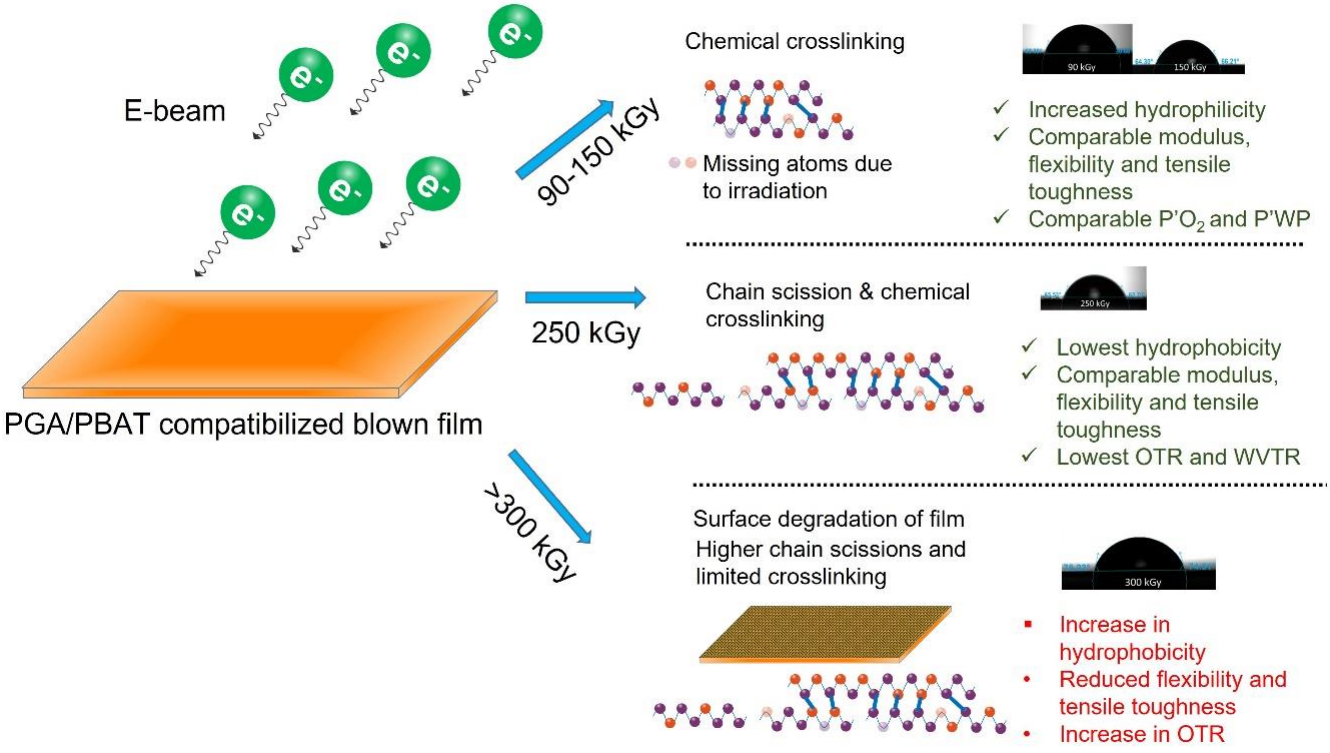

Figure 6: Schematic summary of possible effects (structural and functional) of different dosages of e-beam treatment on the properties of PGA/PBAT compatibilized films.

Table 3. Gas barrier properties showing oxygen transmission rate (OTR), oxygen permeability coefficient ($P'O_2$), water vapor transmission rate (WVTR), and water permeability coefficient (P'WV) for commonly used food packaging materials[35-36] and the materials produced in this work. OTR1 and $P'O_2$1 were conducted at 23 °C / 0 % relative humidity, OTR2 and $P'O_2$ were conducted at 23 °C / 50 % relative humidity, and WVTR and P'WV were conducted at 38 °C / 90 % relative humidity.

Sample	Thickness (µm)	OTR1 (cm^3 m^{-2} 24 h^{-1})	$P'O_2$1 (cm^3 mm m^{-2} 24 $h^{-1}atm^{-1}$)	OTR2 (cm^3 m^{-2} 24 h^{-1})	$P'O_2$2 (cm^3 mm m^{-2} 24 h^{-1} atm^{-1})	WVTR (g m^{-2} 24 h^{-1})	P'WV (g mm m^{-2} 24 h^{-1})
LDPE	20~80	-	98 – 453	-	98 – 453	-	0.5 – 2.0
HDPE	20~80	-	26.3 – 98.5	-	26.3 – 98.5	-	0.1 – 5
PTFE	50	-	222 – 387	-	222 – 387	-	0.0045 – 0.3
PP	20~60	-	35 – 377	-	35 – 377	-	0.2 – 0.4
PGA[37]	20	-	-	-	0.013	-	0.165
PBAT	~50	-	-	-	82.1	-	6.34
0 kGy	101.2 ± 1.6	702.8 ± 80.5	71.1 ± 8.2	734.1 ± 71.1	74.3 ± 7.2	239.8 ± 24.9	24.3 ± 2.5
90 kGy	95.4 ± 3.7	657.8 ± 61.9	62.8 ± 5.9	688.4 ± 70.9	65.7 ± 6.8	275.4 ± 30.9	26.3 ± 2.9
150 kGy	98.2 ± 3.1	619.4 ± 63.9	60.8 ± 6.3	651.1 ± 62.9	63.9 ± 6.2	277.5 ± 25.7	27.3 ± 2.5
250 kGy	113 ± 11.2	504.1 ± 58.2	57.0 ± 6.6	529.1 ± 59.1	59.8 ± 6.7	236.9 ± 26.5	26.8 ± 3.0
300 kGy	123 ± 16.8	565.0 ± 61.5	69.5 ± 7.5	594.8 ± 67.9	73.2 ± 8.3	-	-

Conclusions

The effect of EBT on the surface of GMA compatibilized PGA/PBAT blown films and gas barrier properties for application in packaging was investigated. GMA was shown to act as a compatibilizer by reacting with the chain end groups of PGA and PBAT through epoxide groups, bridging the interface between blend components. This resulted in a high strain, strength, and tough polymer blend. The application of EBT to the surface of the polymer blend film with varying dosage levels up to 450 kGy induced crosslinking up to 250 kGy but degradation above 250 kGy. Below 300 kGy, EBT had a minimal effect on the mechanical properties, with a slight increase in tensile strength from 15.8 to 18.1 MPa and a slight decrease in the strain at break from 577.5 % to 541.2 %. However, degradation caused larger decreases in tensile strength, strain at break, and elastic modulus for 300 kGy and higher dosages. The gas barrier properties of the polymer blend before EBT already exhibited comparable oxygen barrier properties to commonly used polymers for film packaging. EBT at 250 kGy reduced the oxygen permeability of the film by a further 20 %, from 71.1 to 57.0 cm^3 mm m^{-2} 24 h^{-1} atm^{-1}. A slight increase in the water vapor permeability was observed due to the additional crosslinking, potentially due to surface defects, corresponding with the observed increase in hydrophilicity from contact angle measurements. The results from this study pave the way for further research into the use of EBT for polymer films as a route to increasing gas barrier properties for viable alternatives to polymers currently used in food packaging.

Supporting Information

FTIR of (20/80/2) films post e-beam of 450 kGy; SEM of e-beam treated 0 kGy, 90 kGy, 150 kGy and 250 kGy films; Cross section SEM of (20/80) and (20/80/2) films; DSC data; melting and crystallinity information; tensile results; OTR and P'O_2 for 350 kGy, 400 kGy and 450 kGy.

Acknowledgment

The authors acknowledge PJIM Polymer Scientific Co., Ltd. for funding this project. C.W. thanks for supporting the RSC International Exchange Scheme (IEC\NSFC\191291). P.K.S would like to acknowledge Mr. Martin Worrall for his processing insights in blend preparation.

References

(1) Wu, F.; Misra, M.; Mohanty, A. K. Challenges and new opportunities on barrier performance of biodegradable polymers for sustainable packaging. *Progress in Polymer Science* **2021,** *117*, 101395, DOI: https://doi.org/10.1016/j.progpolymsci.2021.101395.
(2) Lebreton, L.; Andrady, A. Future scenarios of global plastic waste generation and disposal. *Palgrave Communications* **2019,** *5* (1), 6, DOI: 10.1057/s41599-018-0212-7.

(3) Samantaray, P. K.; Little, A.; Wemyss, A. M.; Iacovidou, E.; Wan, C. Design and Control of Compostability in Synthetic Biopolyesters. *ACS Sustainable Chemistry & Engineering* **2021,** *9* (28), 9151-9164, DOI: 10.1021/acssuschemeng.1c01424.
(4) Arrieta, M. P.; Samper, M. D.; Aldas, M.; López, J. On the Use of PLA-PHB Blends for Sustainable Food Packaging Applications. *Materials* **2017,** *10* (9), 1008.
(5) Mahmoodi, A.; Ghodrati, S.; Khorasani, M. High-Strength, Low-Permeable, and Light-Protective Nanocomposite Films Based on a Hybrid Nanopigment and Biodegradable PLA for Food Packaging Applications. *ACS Omega* **2019,** *4* (12), 14947-14954, DOI: 10.1021/acsomega.9b01731.
(6) Yusoff, N. H.; Pal, K.; Narayanan, T.; de Souza, F. G. Recent trends on bioplastics synthesis and characterizations: Polylactic acid (PLA) incorporated with tapioca starch for packaging applications. *Journal of Molecular Structure* **2021,** *1232*, 129954, DOI: https://doi.org/10.1016/j.molstruc.2021.129954.
(7) Dammak, M.; Fourati, Y.; Tarrés, Q.; Delgado-Aguilar, M.; Mutjé, P.; Boufi, S. Blends of PBAT with plasticized starch for packaging applications: Mechanical properties, rheological behaviour and biodegradability. *Industrial Crops and Products* **2020,** *144*, 112061.
(8) Zhai, X.; Wang, W.; Zhang, H.; Dai, Y.; Dong, H.; Hou, H. Effects of high starch content on the physicochemical properties of starch/PBAT nanocomposite films prepared by extrusion blowing. *Carbohydrate Polymers* **2020,** *239*, 116231, DOI: https://doi.org/10.1016/j.carbpol.2020.116231.
(9) Xiong, S.-J.; Pang, B.; Zhou, S.-J.; Li, M.-K.; Yang, S.; Wang, Y.-Y.; Shi, Q.; Wang, S.-F.; Yuan, T.-Q.; Sun, R.-C. Economically Competitive Biodegradable PBAT/Lignin Composites: Effect of Lignin Methylation and Compatibilizer. *ACS Sustainable Chemistry & Engineering* **2020,** *8* (13), 5338-5346, DOI: 10.1021/acssuschemeng.0c00789.
(10) Shimpi, N. G. *Biodegradable and Biocompatible Polymer Composites: Processing, Properties and Applications*, Woodhead Publishing, 2017.
(11) Park, C.; Kim, E. Y.; Yoo, Y. T.; Im, S. S. Effect of hydrophilicity on the biodegradability of polyesteramides. *Journal of Applied Polymer Science* **2003,** *90* (10), 2708-2714, DOI: https://doi.org/10.1002/app.12925.
(12) Souza, P. M. S.; Sommaggio, L. R. D.; Marin-Morales, M. A.; Morales, A. R. PBAT biodegradable mulch films: Study of ecotoxicological impacts using Allium cepa, Lactuca sativa and HepG2/C3A cell culture. *Chemosphere* **2020,** *256*, 126985.
(13) Rychter, P.; Kawalec, M.; Sobota, M.; Kurcok, P.; Kowalczuk, M. Study of aliphatic-aromatic copolyester degradation in sandy soil and its ecotoxicological impact. *Biomacromolecules* **2010,** *11* (4), 839-847.
(14) Messin, T.; Marais, S.; Follain, N.; Guinault, A.; Gaucher, V.; Delpouve, N.; Sollogoub, C. Biodegradable PLA/PBS multinanolayer membrane with enhanced barrier performances. *Journal of Membrane Science* **2020,** *598*, 117777, DOI: https://doi.org/10.1016/j.memsci.2019.117777.
(15) Wang, B.; Jin, Y.; Kang, K. e.; Yang, N.; Weng, Y.; Huang, Z.; Men, S. Investigation on compatibility of PLA/PBAT blends modified by epoxy-terminated branched polymers through chemical micro-crosslinking. *epoly* **2020,** *20* (1), 39-54, DOI: doi:10.1515/epoly-2020-0005.
(16) Dong, W.; Zou, B.; Ma, P.; Liu, W.; Zhou, X.; Shi, D.; Ni, Z.; Chen, M. Influence of phthalic anhydride and bioxazoline on the mechanical and morphological properties of biodegradable poly(lactic acid)/poly[(butylene adipate)-co-terephthalate] blends. *Polymer International* **2013,** *62* (12), 1783-1790, DOI: https://doi.org/10.1002/pi.4568.
(17) Wu, N.; Zhang, H. Mechanical properties and phase morphology of super-tough PLA/PBAT/EMA-GMA multicomponent blends. *Materials Letters* **2017,** *192*, 17-20.
(18) Ellingford, C.; Samantaray, P. K.; Farris, S.; McNally, T.; Tan, B.; Sun, Z.; Huang, W.; Ji, Y.; Wan, C. Reactive extrusion of biodegradable PGA/PBAT blends to enhance flexibility and gas barrier properties. *Journal of Applied Polymer Science* **2021,** *n/a* (n/a), 51617, DOI: https://doi.org/10.1002/app.51617.
(19) Samantaray, P. K.; Little, A.; Haddleton, D. M.; McNally, T.; Tan, B.; Sun, Z.; Huang, W.; Ji, Y.; Wan, C. Poly(glycolic acid) (PGA): a versatile building block expanding high performance and

sustainable bioplastic applications. *Green Chemistry* **2020,** *22* (13), 4055-4081, DOI: 10.1039/D0GC01394C.
(20) Yamane, K.; Sato, H.; Ichikawa, Y.; Sunagawa, K.; Shigaki, Y. Development of an industrial production technology for high-molecular-weight polyglycolic acid. *Polymer Journal* **2014,** *46* (11), 769-775.
(21) Wang, R.; Sun, X.; Chen, L.; Liang, W. Morphological and mechanical properties of biodegradable poly(glycolic acid)/poly(butylene adipate-co-terephthalate) blends with in situ compatibilization. *RSC Advances* **2021,** *11* (3), 1241-1249, DOI: 10.1039/D0RA08813G.
(22) Shen, J.; Wang, K.; Ma, Z.; Xu, N.; Pang, S.; Pan, L. Biodegradable blends of poly(butylene adipate-co-terephthalate) and polyglycolic acid with enhanced mechanical, rheological and barrier performances. *Journal of Applied Polymer Science* **2021,** *138* (43), 51285, DOI: https://doi.org/10.1002/app.51285.
(23) Niu, D.; Xu, P.; Sun, Z.; Yang, W.; Dong, W.; Ji, Y.; Liu, T.; Du, M.; Lemstra, P. J.; Ma, P. Superior toughened bio-compostable Poly (glycolic acid)-based blends with enhanced melt strength via selective interfacial localization of in-situ grafted copolymers. *Polymer* **2021,** *235*, 124269.
(24) Burkert, S.; Kuntzsch, M.; Bellmann, C.; Uhlmann, P.; Stamm, M. Tuning of surface properties of thin polymer films by electron beam treatment. *Applied Surface Science* **2009,** *255* (12), 6256-6261, DOI: https://doi.org/10.1016/j.apsusc.2009.01.096.
(25) Kita, H.; Muraoka, M.; Tanaka, K.; Okamoto, K.-i. Permeation of Gases through Electron-Beam-Irradiated Polymer Films. *Polymer Journal* **1988,** *20* (6), 485-491, DOI: 10.1295/polymj.20.485.
(26) Kumar, M.; Mohanty, S.; Nayak, S. K.; Rahail Parvaiz, M. Effect of glycidyl methacrylate (GMA) on the thermal, mechanical and morphological property of biodegradable PLA/PBAT blend and its nanocomposites. *Bioresource Technology* **2010,** *101* (21), 8406-8415, DOI: https://doi.org/10.1016/j.biortech.2010.05.075.
(27) Reis, A. V.; Fajardo, A. R.; Schuquel, I. T.; Guilherme, M. R.; Vidotti, G. J.; Rubira, A. F.; Muniz, E. C. Reaction of glycidyl methacrylate at the hydroxyl and carboxylic groups of poly (vinyl alcohol) and poly (acrylic acid): is this reaction mechanism still unclear? *The Journal of organic chemistry* **2009,** *74* (10), 3750-3757.
(28) Coiai, S.; Di Lorenzo, M. L.; Cinelli, P.; Righetti, M. C.; Passaglia, E. Binary Green Blends of Poly (lactic acid) with Poly (butylene adipate-co-butylene terephthalate) and Poly (butylene succinate-co-butylene adipate) and Their Nanocomposites. *Polymers* **2021,** *13* (15), 2489.
(29) Geisler, M.; Pal, T. S.; Arnhold, K.; Malanin, M.; Müller, M. T.; Voit, B.; Pionteck, J.; Lederer, A. Impact of Electron Beam Irradiation on Thermoplastic Polyurethanes Unraveled by Thermal Field-Flow Fractionation. *Polymer Degradation and Stability* **2021,** *183*, 109423, DOI: https://doi.org/10.1016/j.polymdegradstab.2020.109423.
(30) Madera-Santana, T. J.; Meléndrez, R.; González-García, G.; Quintana-Owen, P.; Pillai, S. D. Effect of gamma irradiation on physicochemical properties of commercial poly(lactic acid) clamshell for food packaging. *Radiation Physics and Chemistry* **2016,** *123*, 6-13, DOI: https://doi.org/10.1016/j.radphyschem.2016.02.001.
(31) Saeki, H. Effects of Heat-Treatment on Electron Beam Sensitivities and Chain Scission Efficiencies of Poly(MMA-co-t-BMA). *Journal of The Electrochemical Society* **1987,** *134* (5), 1194-1199, DOI: 10.1149/1.2100641.
(32) Chen, Y. F.; Zhang, T.; Tang, M.; Xie, D.; Long, Q.; Li, C. Y. The effect of high-current pulsed electron beam modification on the surface wetting property of polyamide 6. *epoly* **2017,** *17* (1), 23-29, DOI: doi:10.1515/epoly-2016-0078.
(33) Pukhova, I. V.; Savkin, K. P.; Laput, O. A.; Lytkina, D. N.; Botvin, V. V.; Medovnik, A. V.; Kurzina, I. A. Effects of ion- and electron-beam treatment on surface physicochemical properties of polylactic acid. *Applied Surface Science* **2017,** *422*, 856-862, DOI: https://doi.org/10.1016/j.apsusc.2017.06.112.

(34) Wang, J.; Gardner, D. J.; Stark, N. M.; Bousfield, D. W.; Tajvidi, M.; Cai, Z. Moisture and Oxygen Barrier Properties of Cellulose Nanomaterial-Based Films. *ACS Sustainable Chemistry & Engineering* **2018,** *6* (1), 49-70, DOI: 10.1021/acssuschemeng.7b03523.
(35) Lange, J.; Wyser, Y. Recent innovations in barrier technologies for plastic packaging—a review. *Packaging Technology and Science* **2003,** *16* (4), 149-158, DOI: https://doi.org/10.1002/pts.621.
(36) Abbott, S. Permeability Calculations. https://www.stevenabbott.co.uk/practical-coatings/permeability.php (accessed 28 January).
(37) Murcia Valderrama, M. A.; van Putten, R. J.; Gruter, G. M. PLGA Barrier Materials from CO2. The influence of Lactide Co-monomer on Glycolic Acid Polyesters. *ACS Appl Polym Mater* **2020,** *2* (7), 2706-2718, DOI: 10.1021/acsapm.0c00315.

GRAPHICAL ABSTRACT

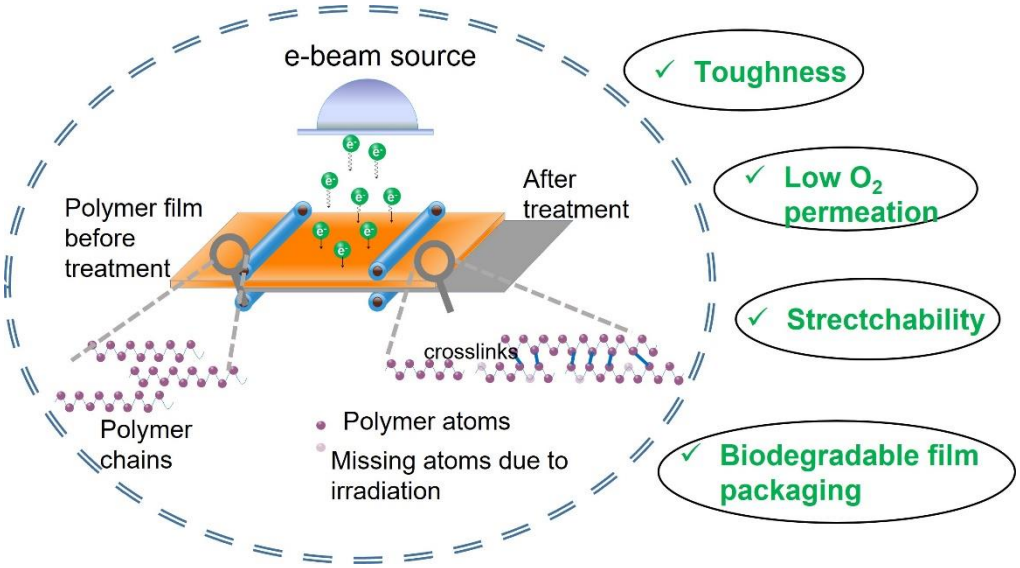

E-beam mediated crosslinking improves the oxygen barrier performance of compostable PGA/PBAT films suitable for flexible food packaging applications